cost and better performance than the M-algorithm [6] for the same computational cost. The performance–complexity tradeoff of all the demodulators in Figs. 4 and 5 can be improved by employing (unbiased) MMSE preprocessing [10], [18], but the relative tradeoffs remain qualitatively similar. The relative tradeoffs after fewer than four demodulation–decoding iterations are also qualitatively similar.

VI. Conclusion

We have proposed a tree-search algorithm for list-based MIMO soft demodulation. The proposed algorithm is based on the "best-first" search principle used in the stack algorithm, but rather than applying that principle to a single (global) stack, the global stack is partitioned into a stack for each level of the tree, and the algorithm sequentially proceeds by performing one best-first search step in each of these stacks in the natural ordering of the tree. By assigning appropriate priorities to the level at which this best-first search per level processing restarts once a leaf node has been obtained, we have shown that the proposed approach can achieve a performance–complexity tradeoff that dominates those of the stack (LISS) algorithm in [2], the list sphere decoder [1], and the M-algorithm [6] in the low-complexity region.

References

[1] B. M. Hochwald and S. ten Brink, "Achieving near-capacity on a multiple-antenna channel," *IEEE Trans. Commun.*, vol. 51, no. 3, pp. 389–399, Mar. 2003.

[2] S. Baro, J. Hagenauer, and M. Witzke, "Iterative detection of MIMO transmission using a list-sequential (LISS) detector," in *Proc. IEEE Int. Conf. Commun.*, Anchorage, AK, May 2003, vol. 4, pp. 2653–2657.

[3] J. Hagenauer and C. Kuhn, "The list-sequential (LISS) algorithm and its application," *IEEE Trans. Commun.*, vol. 55, no. 5, pp. 918–928, May 2007.

[4] J. Boutros, N. Gresset, L. Brunel, and M. Fossorier, "Soft-input soft-output lattice sphere decoder for linear channels," in *Proc. IEEE Global Telecomm. Conf.*, San Francisco, CA, Dec. 2003, vol. 3, pp. 1583–1587.

[5] H. Vikalo, B. Hassibi, and T. Kailath, "Iterative decoding for MIMO channels via modified sphere decoding," *IEEE Trans. Wireless Commun.*, vol. 3, no. 6, pp. 2299–2311, Nov. 2004.

[6] Y. L. C. de Jong and T. J. Willink, "Iterative tree search detection for MIMO wireless systems," *IEEE Trans. Commun.*, vol. 53, no. 6, pp. 930–935, Jun. 2005.

[7] S. Bittner, E. Zimmermann, W. Rave, and G. Fettweis, "List sequential MIMO detection: Noise bias term and partial path augmentation," in *Proc. IEEE Int. Conf. Commun.*, Istanbul, Turkey, Jun. 2006, pp. 1300–1305.

[8] D. J. Love, S. Hosur, A. Batra, and R. W. Heath, Jr., "Space–time Chase decoding," *IEEE Trans. Wireless Commun.*, vol. 4, no. 5, pp. 2035–2039, Sep. 2005.

[9] J. Luo, K. R. Pattipati, P. Willett, and G. M. Levchuk, "Fast optimal and suboptimal any-time algorithms for CDMA multiuser detection based on branch and bound," *IEEE Trans. Commun.*, vol. 52, no. 4, pp. 632–642, Apr. 2004.

[10] A. D. Murugan, H. El Gamal, M. O. Damen, and G. Caire, "A unified framework for tree search decoding: Rediscovering the sequential decoder," *IEEE Trans. Inf. Theory*, vol. 52, no. 3, pp. 933–953, Mar. 2006.

[11] J. Anderson and S. Mohan, "Sequential coding algorithms: A survey and cost analysis," *IEEE Trans. Commun.*, vol. COM-32, no. 2, pp. 169–176, Feb. 1984.

[12] B. Hassibi and B. Hochwald, "High-rate codes that are linear in space and time," *IEEE Trans. Inf. Theory*, vol. 48, no. 7, pp. 1804–1824, Jul. 2002.

[13] R. A. Horn and C. R. Johnson, *Matrix Analysis*. New York: Cambridge Univ. Press, 1985.

[14] P. Chevillat and D. Costello, Jr., "A multiple stack algorithm for erasurefree decoding of convolutional codes," *IEEE Trans. Commun.*, vol. COM-25, no. 12, pp. 1460–1470, Dec. 1977.

[15] G. J. Foschini, G. Golden, R. Valenzuela, and P. Wolniansky, "Simplified processing for high spectral efficiency wireless communication employing multi-element arrays," *IEEE J. Sel. Areas Commun.*, vol. 17, no. 11, pp. 1841–1852, Nov. 1999.

[16] F. Hasegawa, J. Luo, K. R. Pattipati, P. Willett, and D. Pham, "Speed and accuracy comparison of techniques for multiuser detection in synchronous CDMA," *IEEE Trans. Commun.*, vol. 52, no. 4, pp. 540–545, Apr. 2004.

[17] M. Nekuii, "Soft demodulation schemes for MIMO communication systems," Ph.D. dissertation, McMaster Univ., Hamilton, ON, Canada, Aug. 2008.

[18] E. Zimmermann and G. Fettweis, "Unbiased MMSE tree search detection for multiple antenna systems," in *Proc. Int. Symp. Wireless Pers. Multimedia Commun.*, San Diego, CA, Sep. 2006.

Wireless Access Point Voice Capacity Analysis and Enhancement Based on Clients' Spatial Distribution

Ahmed Shawish, *Student Member, IEEE*, Xiaohong Jiang, *Member, IEEE*, Pin-Han Ho, *Member, IEEE*, and Susumu Horiguchi, *Senior Member, IEEE*

***Abstract*—An efficient voice-over-IP (VoIP) support at the wireless access point (AP) of a wireless LAN (WLAN) remains a challenge for the last-mile wireless coverage of IP networks with mobility support. Due to the limited bandwidth that is available in WLANs, an accurate analysis of the voice capacity in such networks is crucial for the efficient utilization of their resources. The available analytical models only provide the upper and lower bounds on voice capacity, which may significantly overestimate or underestimate the WLAN's capability of supporting VoIP and, thus, are not suitable for the mentioned purpose. In this paper, we focus on the voice capacity analysis of a wireless 802.11(a/b) AP running the distributed coordination function (DCF). In particular, we show that by incorporating the clients' spatial distribution into the analysis, we are able to develop a new analytical model for a much more accurate estimation of the average voice capacity. By properly exploring this spatial information, we further propose a new scheme for AP placement such that the overall voice capacity can be enhanced. The efficiency of the new voice capacity model and the new AP placement scheme is validated through both analytical and simulation studies.**

***Index Terms*—IEEE 802.11 distributed coordination function (DCF), spatial distribution, voice capacity, voice over IP (VoIP), wireless access point (AP).**

I. Introduction

Voice over Internet Protocol (VoIP) is one of the fastest-growing Internet applications due to its cost efficiency and its promising ability to merge voice communication with other multimedia and data applications [1]. Driven by the huge demands for flexible connectivity and portable access at reduced costs, wireless local area networks (WLANs) are increasingly making their way into residential, commercial, industrial, and public areas. While the majority of traffic in WLAN are data, it is expected that the voice application will become

Manuscript received February 12, 2008; revised July 2, 2008. First published September 9, 2008; current version published May 11, 2009. The review of this paper was coordinated by Prof. R. Jäntti.

A. Shawish is with the Graduate School of Information Sciences, Tohoku University, Sendai 980-8579, Japan, and also with the Faculty of Computer and Information Sciences, Ain Shams University, Cairo 11566, Egypt (e-mail: ahmedmg@ecei.tohoku.ac.jp).

X. Jiang and S. Horiguchi are with the Graduate School of Information Sciences, Tohoku University, Sendai 980-8579, Japan (e-mail: jiang@ecei.tohoku.ac.jp; susumu@ecei.tohoku.ac.jp).

P.-H. Ho is with the Department of Electrical and Computer Engineering, University of Waterloo, Waterloo, ON N2L 3G1, Canada (e-mail: pinhan@bbcr.uwaterloo.ca).

Digital Object Identifier 10.1109/TVT.2008.2005523

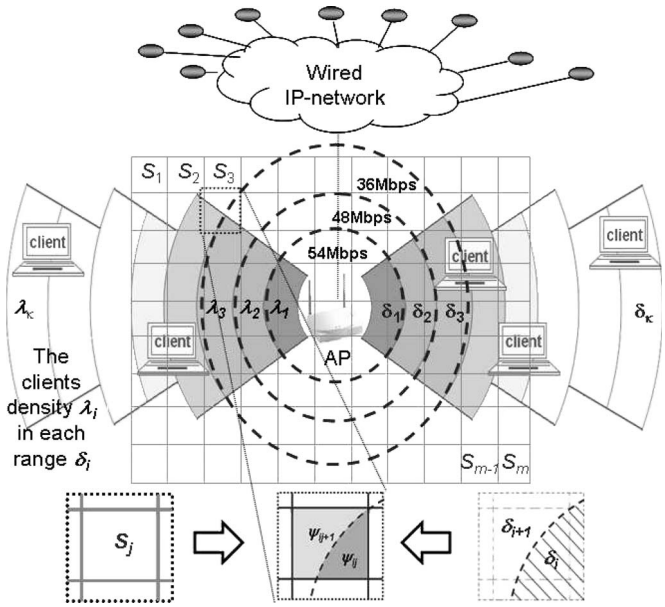

Fig. 1. The 802.11a transmission rates.

a significant driver for the deployment of WLANs, which is evident from the rapid flourish of VoIP applications in recent years.

When designing a voice-over-WLAN system, the most important parameter of concern is the voice capacity of the wireless access point (AP), which is defined as the number of voice connections that can simultaneously be supported through the AP. Since the current WLANs have a very limited bandwidth, and the voice admission control there mainly depends on this parameter to accept or reject new voice calls [2], a careful voice capacity analysis is crucial for the efficient utilization of WLAN's resources.

The available models for voice capacity analysis only provide the upper and lower bounds on voice capacity [3]–[8], because they were developed based on the assumption that the transmission rate (R) between the AP and any client in WLAN is always either the maximum or the minimum achievable rate. In practice, however, R varies depending on the access distance, shadowing effect, and channel fading along the signal path [9]. Thus, the maximum R is only available for those clients who are very close to the AP, whereas R is sharply stepped down (nonlinearly) as the access distance increases, as illustrated in Fig. 1 for the 802.11a protocol.[1] Therefore, the available simple models may significantly overestimate or underestimate the voice capacity.

In this paper, we focus on the voice capacity analysis and the enhancement of distributed coordination function (DCF)-based IEEE 802.11a/b WLANs. The main contributions of this paper are the following.

1) Considering the clients' spatial distribution (CSD), we develop a new analytical model for a much more accurate estimation of WLANs' voice capacity.
2) By properly exploring the CSD information, we further propose a new scheme for AP placement such that the overall voice capacity can be enhanced.
3) We demonstrate through our new model and scheme that the CSD has a significant implication on the achievable voice capacity, and thus, it should carefully be considered in the AP placement.

[1]In practice, due to other factors like channel fading, shadowing effect, etc, the signal transmission rate reduction may not exactly follow the very regular pattern shown in Fig. 1. Fig. 1 is mainly used for illustration here.

The rest of this paper is organized as follows. Section II introduces the background and related work. In Section III, we develop an analytical model to estimate the voice capacity based on the CSD. In Section IV, we introduce a new scheme for voice capacity enhancement. Section V presents the validation of our model and scheme. Finally, we conclude this paper in Section VI.

II. Background and Related Work

In this section, we introduce the IEEE 802.11 DCF-based WLAN and the voice capacity of WLAN.

A. IEEE 802.11 DCF-Based WLAN

The basic access method in IEEE 802.11 WLANs is the DCF, which is based on carrier-sense multiple accesses with collision avoidance. In the DCF, all the clients with packets that are ready for transmission observe the shared medium before attempting to transmit. If the medium is sensed busy, the clients delay the transmission until the medium is sensed idle for the period of a DCF interframe space (DIFS). The clients then enter the backoff phase, in which every client chooses a random backoff counter from $[0, CW_{\min}]$ (where $CW_{\min}$ is the minimum contention window size). The backoff counter decreases by 1 for every idle timeslot and freezes if the channel is sensed busy. The decrement procedure is resumed after the channel is sensed idle again for a period of DIFS. The client transmits the packet when the backoff counter reaches 0. If the packet is successfully received, then the receiver transmits an ACK following a short interframe space (SIFS). In case of a failed transmission due to collision or transmission error, the sender may attempt to retransmit his packet for a specific number of trials before it is dropped, where the contention window size is doubled for each trial until it reaches the maximum value $(CW_{\max})$. Following every successful transmission, the contention window size is reset to its initial (minimal) value.

B. Voice Capacity of WLAN

The available analysis on the WLANs' voice capacity has been conducted via both experiments in [3]–[5] and analytical models in [6]–[8]. Based on a testbed, [3] shows that the 802.11b can only support ten voice connections by adopting G.711 voice codecs, 10-ms audio payload, and silence suppression. A measurement experiment without silence suppression was carried out in [4], which indicates that only six voice connections can be accommodated. In [5], it has been shown that the 802.11b can support up to 10 G.711 and 18 G.723.1 voice connections with 20 and 30 ms of audio payload, respectively. In general, the available measurement results indicate that the silence suppression and the audio payload interval heavily affect the voice capacity. These experiments, however, can only be considered as case studies and may not generally be applicable.

On the analytical model side, the model in [6] considers the overheads (e.g., the voice packet header, DIFS, SIFS, ACK packet, and random backoff) and simplifies the voice capacity analysis with the assumption that there are no collisions. In [7], another better analytical model was proposed by assuming that there are always two active stations competing for the wireless channel. In [8], the authors improved the previous models by considering both the details of collision avoidance mechanism and the practical AP bottleneck effect induced by the unbalanced traffic of AP/clients. Although the available models successfully quantified the factors that affect the voice capacity, like overheads, unbalance traffic load, and collision, they can only provide the theoretical upper or lower bounds on the voice capacity since they always assume a constant transmission rate (either the maximum or the minimum) in their analysis.

III. Analytical Modeling for Voice Capacity

In this section, we introduce the voice capacity analysis and also our new approach for it.

A. Voice Capacity Analysis

To analyze the AP's voice capacity, we first need to understand the maximum channel throughput that can be achieved in the AP, as modeled in [6] and [7], that is,

$$\frac{T_P \cdot R_{\text{avg}}}{T_{\text{voice}} + T_{\text{Ack}} + T_{\text{SIFS}} + T_{\text{DIFS}} + T_{\text{Backoff}}}. \tag{1}$$

The foregoing equation indicates that the channel throughput is a function of the AP's average transmission rate R_{avg} and other parameters like the time T_P needed to transmit the voice payload, the time T_{voice} needed to transmit the whole voice packet, the SIFS time T_{SIFS}, the DIFS time T_{DIFS}, the time T_{Ack} needed to transmit the acknowledgment packet, and the backoff time overhead T_{Backoff}.

For an IEEE 802.11 WLAN, T_{SIFS} and T_{DIFS} in (1) are usually constants, whereas $T_P = S_P/R_{\text{avg}}$, $T_{\text{voice}} = T_{\text{PHY}} + ((S_{\text{MAC}} + S_h + S_P)/R_{\text{avg}})$, and $T_{\text{Ack}} = T_{\text{PHY}} + (S_A/R_{\text{avg}})$ are determined by other basic parameters. S_{MAC}, S_h, and S_P are the sizes of the voice packet medium access control (MAC) header, real-time transport protocol/user datagram protocol/IP header, and voice payload, respectively. S_A and T_{PHY} are the Ack packet size and the time needed to process the physical layer overhead, respectively. Finally, T_{Backoff} in (1) can be evaluated based on the following formula with the consideration of collision [7]:

$$T_{\text{Backoff}} = \begin{cases} 4.5\times 9 + T_w \times 0.06\ \mu\text{s}, & \text{for IEEE 802.11a WLAN} \\ 8.5\times 20 + T_w \times 0.03\ \mu\text{s}, & \text{for IEEE 802.11b WLAN} \end{cases}$$

where T_w is defined in terms of the basic parameters as

$$T_w = T_{\text{SIFS}} + T_{\text{DIFS}} + 2T_{\text{PHY}} + \frac{1}{R_{\text{avg}}}(S_H + S_P + S_A + S_{\text{MAC}}).$$

The typical values for the preceding basic parameters (except R_{avg}) are shown in Table I(a) when the IEEE 802.11a/b standards are considered.

Based on the preceding channel throughput model, the voice capacity C of the AP (i.e., the number of VoIP connections the AP can simultaneously support) can be estimated as in (2), shown at the bottom of the page, where all the voice calls are assumed to use the same voice codec with a bit rate of L bits per second.

Based on (2), the maximum numbers of voice calls that a single AP can support under different transmission rates and payload size are illustrated in Fig. 2. The figure clearly indicates that the voice capacity C is significantly affected by the variation of R_{avg}. For example, the IEEE 802.11a WLAN can support up to 92 G.729 voice connections (with 30 ms payload size) if R_{avg} is equal to 54 Mb/s. This capacity is dramatically decreased to 48 if R_{avg} decrease to 6 Mb/s. Therefore, an accurate model of R_{avg} is crucial for the efficient estimation of the voice capacity in WLAN.

TABLE I
IEEE 802.11(a/b) DCF-Based WLAN Parameters and CSD Patterns

Part	Item	802.11b	802.11a
a)	Transmission rates R	11, 5.5, 2, and 1Mbps	54, 48, 36, 24, 18, 12, 9, and 6Mbps
	Slot Time	20μs	9μs
	T_{SIFS}	10μs	16μs
	T_{DIFS}	50μs	34μs
	CW_{min}	32	16
	CW_{max}	1024	1024
	Retry Limit	7	7
	T_{PHY}	192μs	24μs
	S_{MAC}	(34 Byte × 8)	
	S_H	(40 Byte × 8)	
	S_P	(payload × 8)	
	S_A	(14 Byte × 8)	
b)	Pattern1	$(\lambda_1,...,\lambda_4)$= (79,52,39,30)	$(\lambda_1,...,\lambda_8)$=(25,54, 28,24,20,19,16,14)
	Pattern2	$(\lambda_1,...,\lambda_4)$= (10,46,95,49)	$(\lambda_1,...,\lambda_8)$=(2,8,11, 35,60,35,27,22)
	Pattern3	$(\lambda_1,...,\lambda_4)$= (8,14,25,153)	$(\lambda_1,...,\lambda_8)$=(2,6,6,8, 10,15,53,100)

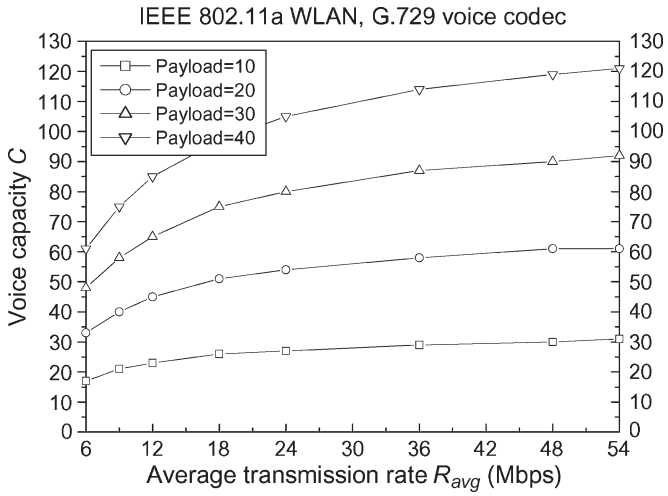

Fig. 2. Voice capacity of 802.11a under different R_{avg}.

B. New Model for R_{avg}

For an accurate estimation for R_{avg}, we first need to characterize the spatial distribution of the clients. Given a WLAN coverage area, we use a grid to equally divide it into m squares $(S_1, S_2, \ldots, S_m)$, as illustrated in Fig. 1. Supposing that the number of clients N_{S_j} in square S_j $(j = 1, 2, \ldots, m)$ follows the Poisson distribution[2] with a mean value of λ_{S_j}, and that these clients N_{S_j} are uniformly distributed

[2]In practice, due to the mobility of clients in WLAN, they may randomly enter and leave a square independent of each other. Therefore, the number of clients in a square can generally be regarded as a random process similar to the random occurrence of an event per a specified region, which can nicely be described by a Poisson distribution. That is why the Poisson distribution assumption has widely been adopted to describe the number of mobile clients in a specified area [10], [11].

$$C = \left\lfloor \frac{S_P \cdot R_{\text{avg}}}{2L \cdot ((S_H + S_P + S_A + S_{\text{MAC}}) + R_{\text{avg}}(2T_{\text{PHY}} + T_{\text{SIFS}} + T_{\text{DIFS}} + T_{\text{Backoff}}))} \right\rfloor \tag{2}$$

inside the square,[3] then the spatial distribution of the clients in the WLAN area can be described in terms of $(\lambda_{S_1}, \lambda_{S_2}, \ldots, \lambda_{S_m})$.

The step down of the transmission rate in one of the AP's coverage area virtually creates multiple mutually exclusive rate ranges $(\delta_1, \ldots, \delta_k)$ around it (please refer to Fig. 1), where each range δ_i has a particular transmission rate r_i, $i = 1, \ldots, k$. A number of models have been developed to predict the distance limit of each r_i for a given AP (see, for example, [14] and [15]). Thus, the area size of each delta range δ_i can easily be calculated by treating these distance limits as the radius of multiple overlapped circles sharing the same center point (i.e., the AP).

Let ψ_{ij} denote the intersection between δ_i and S_j, that is,

$$\psi_{ij} = S_j \cap \delta_i, \qquad \text{for } 1 \le i \le k, \quad 1 \le j \le m. \tag{3}$$

Then, each δ_i can be expressed in terms of ψ_{ij} as

$$\delta_i = \cup_{j=1}^{m} \psi_{ij}, \quad \text{for } i = 1, \ldots, k. \tag{4}$$

We denote the number of clients in ψ_{ij} by $N_{\psi_{ij}}$. Since the clients are uniformly distributed inside a square S_j, then $N_{\psi_{ij}}$ also follows the Poisson distribution with the mean value $\lambda_{\psi_{ij}}$ determined as

$$\lambda_{\psi_{ij}} = \frac{|\psi_{ij}|}{|S_j|} \times \lambda_{S_j} \tag{5}$$

where $|S|$ denotes the size of area S. We denote the total number of clients in the range δ_i by $N_i = \sum_{j=1}^{m} N_{\psi_{ij}}$. Based on the statistical property of the Poisson distribution, the random variable N_i also follows the Poisson distribution with the mean value $\lambda_i = \sum_{j=1}^{m} \lambda_{\psi_{ij}}$. Thus, the spatial distribution defined in terms of $(\lambda_{S_1}, \lambda_{S_2}, \ldots, \lambda_{S_m})$ is now transformed into $(\lambda_1, \lambda_2, \ldots, \lambda_k)$. If we further denote the total number of clients in the coverage area of the AP by $N (N = \sum_{i=1}^{k} N_i)$, then we can easily prove that the random variable N also follows the Poisson distribution with the mean value $\lambda = \sum_{i=1}^{k} \lambda_i$. Before presenting the main result about the R_{avg} of an AP, we first establish the following lemma about a property of the random variable N.

Lemma 1: For any set of nonnegative variables $x_i \ge 0$, $i = 1, \ldots, k$, let $X = \sum_{i=1}^{k} x_i$. Then, we have

$$\Pr(N_1 = x_1, \ldots, N_k = x_k | N = X) = \frac{X!}{x_1! \cdots x_k!} \prod_{i=1}^{k} \left(\frac{\lambda_i}{\lambda}\right)^{x_i}. \tag{6}$$

Proof: Notice that N_i follows the Poisson distribution with the mean value $\lambda_i = \sum_{j=1}^{m} \lambda_{\psi_{ij}}$ $(i = 1, \ldots, k)$. Then, N_i is distributed as

$$\Pr(N_i = x_i) = \frac{e^{-\lambda_i} \lambda_i^{x_i}}{x_i!}. \tag{7}$$

The mutual independence of N_i's indicates that their joint probability distribution is given by

$$\begin{aligned} \Pr(N_1 = x_1, \ldots, N_k = x_k) &= \prod_{i=1}^{k} \frac{e^{-\lambda_i} \lambda_i^{x_i}}{x_i!} \\ &= e^{-\lambda} \prod_{i=1}^{k} \frac{\lambda_i^{x_i}}{x_i!} \end{aligned} \tag{8}$$

[3]When a square is small enough, the client distribution in it can nicely be approximated as uniform.

where $\lambda = \sum_{i=1}^{k} \lambda_i$. Since the random variable N also follows the Poisson distribution with the mean value λ, then we have

$$\begin{aligned} &\Pr(N_1 = x_1, \ldots, N_k = x_k | N = X) \\ &\quad = \frac{\Pr(N_1 = x_1, \ldots, N_k = x_k)}{\Pr(N = X)} \\ &\quad = \left(e^{-\lambda} \prod_{i=1}^{k} \frac{\lambda_i^{x_i}}{x_i!}\right) \Big/ \left(\frac{e^{-\lambda} \lambda^X}{X!}\right) \\ &\quad = \frac{X!}{x_1 \cdots x_k!} \prod_{i=1}^{k} \left(\frac{\lambda_i}{\lambda}\right)^{x_i}. \end{aligned}$$

■

Based on the preceding lemma, we now can establish the following theorem regarding the evaluation of R_{avg} for an AP.

Theorem 1: Given a WLAN AP with k mutually exclusive rate ranges δ_i $(i = 1, \ldots, k)$, suppose that the transmission rate and the expected number of clients for the range δ_i are r_i and λ_i, respectively. Then, the average transmission rate R_{avg} of this AP can be estimated as

$$\begin{aligned} R_{\text{avg}} = \sum_{X=1}^{\infty} \frac{e^{-\lambda} \lambda^X}{X!} \sum_{\substack{x_1, \ldots, x_k \ge 0 \\ x_1 + \cdots + x_k = X}} &\left(\frac{X!}{x_1 \cdots x_k!} \prod_{i=1}^{k} \left(\frac{\lambda_i}{\lambda}\right)^{x_i}\right) \\ &\cdot \left(\frac{1}{X} \sum_{i=1}^{k} x_i \cdot r_i\right) \end{aligned} \tag{9}$$

where $\lambda = \sum_{i=1}^{k} \lambda_i$.

Proof: Based on the definition of the random variable N, we have

$$R_{\text{avg}} = \sum_{X=1}^{\infty} F(R_{\text{avg}} | N = X) \cdot \Pr(N = X) \tag{10}$$

where $F(R_{\text{avg}} | N = X)$ is the average transmission rate of the AP when there are in total X users in its coverage area. $F(R_{\text{avg}} | N = X)$ can further be expressed as

$$\begin{aligned} &F(R_{\text{avg}} | N = X) \\ &\quad = \sum_{\substack{x_1, \ldots, x_k \ge 0 \\ x_1 + \cdots + x_k = X}} F(R_{\text{avg}} | N_1 = x_1, \ldots, N_k = x_k) \\ &\qquad \cdot \Pr(N_1 = x_1, \ldots, N_k = x_k | N = X). \end{aligned} \tag{11}$$

Based on the assumption that each client, regardless of its location, has the same chance to establish a connection with the AP, then the average transmit rate R_{avg} can easily be evaluated by the following formula given that $N_1 = x_1, \ldots, N_k = x_k$:

$$\begin{aligned} F(R_{\text{avg}} | N_1 = x_1, \ldots, N_k = x_k) &= \sum_{i=1}^{k} \frac{x_i}{x_1 + \cdots + x_k} \cdot r_i \\ &= \frac{1}{X} \sum_{i=1}^{k} x_i \cdot r_i. \end{aligned} \tag{12}$$

Based on Lemma 1 and (12), we can see that $F(R_{\text{avg}}|N=X)$ is given by

$$F(R_{\text{avg}}|N=X)=\sum_{\substack{x_1,\ldots,x_k\geq 0\\ x_1+\cdots+x_k=X}}\left(\frac{1}{X}\sum_{i=1}^{k}x_i\cdot r_i\right)\cdot\left(\frac{X!}{x_1\cdots x_k!}\prod_{i=1}^{k}\left(\frac{\lambda_i}{\lambda}\right)^{x_i}\right). \quad (13)$$

Substituting (13) into (10), we can see that R_{avg} is determined by (9). ■

IV. New Scheme for AP Placement

With the help of CSD, we propose here an AP placement scheme for voice capacity enhancement.

A. Motivation

At the time of building a new WLAN, the network designers usually select the geometric center of the considered area to place the AP. As we will show in the next section, R_{avg} is heavily affected by the CSD. Notice that, in practice, the clients in an area may nonuniformly be distributed (please refer to Fig. 6 for illustration), so its geometric center may be far from the squares with high client density. Therefore, placing the AP at the geometric center of such an area may significantly degrade R_{avg} and thus result in a waste of the WLAN's limited resources. It is notable, however, that some recent studies [16], [17] clearly indicate that despite the diversity of the individual's mobility, the human's mobility pattern in an area (like urban) is actually predictable and stable. Based on the preceding observations, we propose here a new scheme for AP placement based on a careful consideration of the CSD.

B. Proposed Scheme

The main idea of the new scheme is to place the AP as near as possible to the squares with higher client densities such that the average voice capacity can be enhanced as much as possible. By regarding each square's density as a mass point located at the center of the square, this AP placement problem is actually similar to the typical problem of finding the center of gravity (CG) for a set of point masses [13]. The CG for a collection of masses is the point where all the weight of these masses can be considered to be concentrated, and this CG usually does not coincide with their intuitive geometric center. It is notable that to balance the forces that simultaneously act on all the masses, the CG is naturally nearer to the points with heavier masses.

For a collection of point masses $M_1,\ldots,M_m$ located at $(x_1,y_1),\ldots,(x_m,y_m)$, respectively, let $(x_{\text{cg}},y_{\text{cg}})$ denote the coordinate of their CG. Then, the summation of all the gravitational torques created by these masses must be equal to the opposite torque at $(x_{\text{cg}},y_{\text{cg}})$ to balance the forces that simultaneously act on all the masses. Denoting by g the constant of gravity, the torque at a point (x,y) with mass M is equal to the force $M\cdot g$ times the distance from the axis of rotation [13]. Thus, we have

$$\left(\sum_{j=1}^{m}M_j\right)gx_{\text{cg}}=\sum_{j=1}^{m}M_jgx_j$$
$$\left(\sum_{j=1}^{m}M_j\right)gy_{\text{cg}}=\sum_{j=1}^{m}M_jgy_j.$$

The foregoing equalities imply that the torque about the origin would be the same if the entire weight acted through the CG instead of acting through the individual masses. Solving the x and y coordinates of the CG, we have

$$x_{\text{cg}}=\frac{\sum_{j=1}^{m}M_jx_j}{\sum_{j=1}^{m}M_j}\quad y_{\text{cg}}=\frac{\sum_{j=1}^{m}M_jy_j}{\sum_{j=1}^{m}M_j}.$$

Inspired by the preceding typical CG problem, we propose here the following scheme for AP placement (or equally for determining the coordinate $(x_{\text{AP}},y_{\text{AP}})$ for the AP).

AP Placement $(x_{\text{AP}},y_{\text{AP}})$

1) Use a grid to equally divide the WLAN area into squares S_j, $j=1,\ldots,m$.
2) Acquire the expected average number of clients λ_j in square S_j.
3) Determine the coordinate (x_j,y_j) for the center of S_j.
4) Determine (x_{AP}) and (y_{AP}) as

$$x_{\text{AP}}=\sum_{j=1}^{m}\lambda_jx_j/\sum_{j=1}^{m}\lambda_j\quad y_{\text{AP}}=\sum_{j=1}^{m}\lambda_jy_j/\sum_{j=1}^{m}\lambda_j.$$

5) Place AP at $(x_{\text{AP}},y_{\text{AP}})$.

In the next section, the voice capacity enhancement from using the preceding scheme will be demonstrated.

V. Numerical Results

In this section, we first verify the efficiency of the new voice capacity model through simulation. Then, we demonstrate the voice capacity enhancement through using the new AP placement scheme.

A. Simulation Settings

Our simulation is based on the topology shown in Fig. 1. We developed simulators for DCF-based IEEE 802.11a/b WLANs with the basic parameters defined in Table I(a). The three CSD patterns considered in our simulation are illustrated in Fig. 6, where each pattern is stored in a database in the form of a 2-D array of cells.[4] Their corresponding data of the average number of clients λ_i in each range δ_i, which are derived based on the method in Section III, are summarized in Table I(b). The transmission rate R in IEEE 802.11a and IEEE 802.11b WLANs is stepped down every 10 and 20 m, respectively. With respect to the voice codec, we adopt G.711 and G.729 with a variety of payload sizes (10, 20, 30, and 40 ms).

B. Effect of Square Sizing

To understand how the grid's square size affects the estimation efficiency of our new voice capacity model, we conducted both simulation and analytical analysis on an IEEE 802.11a WLAN when a different square size is adopted. The G.729 voice codec with 30-ms payload size was used, and the clients were spatially distributed in WLAN according to patterns 1 and 2 illustrated in Fig. 6. We conducted our analysis by first regarding the whole WLAN's coverage area A as one big square $(m=1)$, and then, we gradually divide it into multiple equal-sized squares $(m=4,9,16,25,\ldots,$ etc), where the analytical estimation of the voice capacity is performed for each value of m until the analytical and numerical results are matched. The corresponding results are summarized in Fig. 3.

We can easily see from Fig. 3 that the number of squares m (or equally the square size A/m) can significantly affect the efficiency of our model for the estimation of the voice capacity. For example, for

[4]The cells are small enough such that each cell contains a maximum of one client.

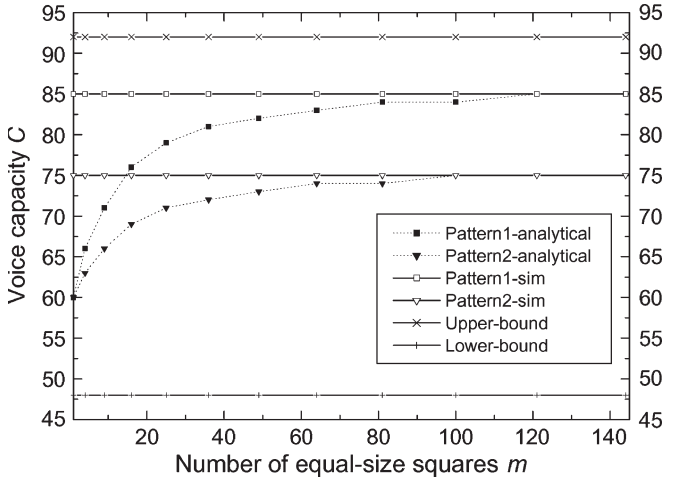

Fig. 3. Voice capacity of 802.11a under different square sizes.

pattern 1, where the actual voice capacity is 85, the estimation of our model is enhanced from 60 to 82 as m increases from 1 to 49 (i.e., A is divided into $7 \times 7 = 49$ equal-sized squares). The results in this figure also clearly indicate that when the square size A/m is small enough (or equally when the number of squares m is larger enough), the number of clients can be regarded as uniformly distributed in a square, and thus, our model can always result in a very efficient estimation of the actual voice capacity. However, for a given estimation error of voice capacity, how to find the minimum number of required m is a complex issue since it is determined by many factors, like the overall area A, the total number of users in the WLAN, how these users are distributed in this area, etc. Nevertheless, compared to the old upper and lower bound models, the estimation efficiency of the voice capacity can significantly be improved by adopting our model even with a rough partition of A.

C. Model Verification

Figs. 4 and 5 show the numerical and analytical results for the IEEE 802.11a/b WLANs' voice capacity under different CSD patterns. For comparison, we also show in both figures the results of the upper and lower bounds. The two figures clearly show that with the help of the CSD information, our analytical model is able to provide a very efficient estimation of the real voice capacity, whereas the corresponding estimations from the available upper and lower bounds are too far from the real case. For example, for the IEEE 802.11a WLAN with G.711 voice codec and 30-ms payload, the voice capacity's upper and lower bounds are 76 and 26, respectively, whereas the numerical and analytical results under the first CSD pattern are 65 and 63, respectively. Similarly, in case of the IEEE 802.11b WLAN with G.729 voice codec and 30-ms payload, the voice capacity's upper and lower bounds are 22 and 9, respectively, whereas the numerical and analytical results under the third CSD pattern are 12 and 13, respectively. The preceding results indicate that the CSD can significantly affect the R_{avg}, so it should carefully be considered for an accurate estimation of the actual voice capacity.

D. Voice Capacity Enhancement

To demonstrate the efficiency of the proposed scheme for AP placement, we studied the three different CSD patterns illustrated in Fig. 6, where the accumulation of the client density with respect to the X- and Y-axes is also shown. Without losing generality, we conducted

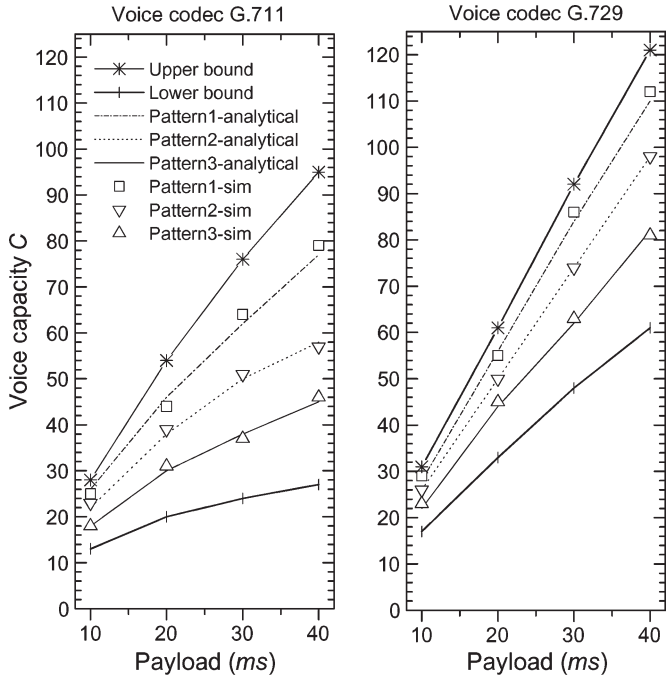

Fig. 4. Voice capacity comparison between analytical and simulation results for 802.11a WLAN.

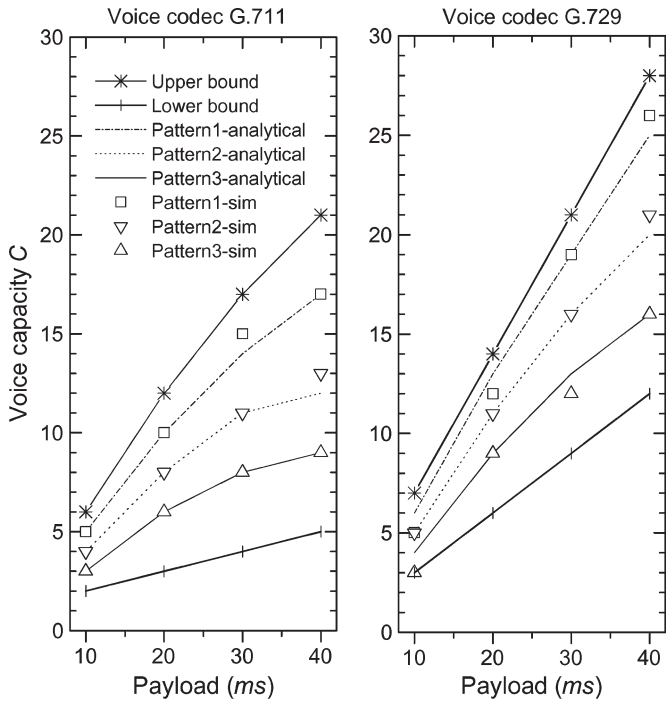

Fig. 5. Voice capacity comparison between analytical and simulation results for 802.11b WLAN.

our study based on an IEEE 802.11a WLAN with G.729 voice codec and 30-ms payload. The implementation results of our proposed scheme are summarized in Fig. 6. For comparison, we also include in that figure the corresponding results when AP is always placed at its geometric center regardless of the CSD. It is notable that the proposed scheme can always result in a voice capacity enhancement for any CSD pattern here, particularly when clients are unsymmetrically distributed

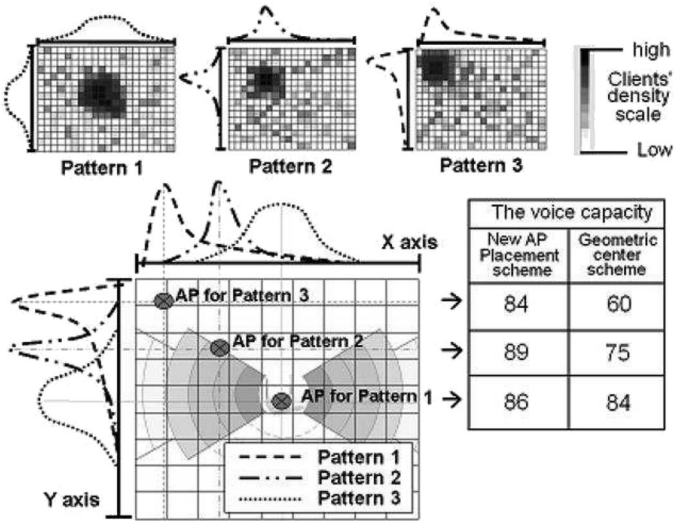

Fig. 6. AP placement under different CSDs.

in the WLAN coverage area. For example, for the first and second (asymmetric) patterns, the voice capacity improvements are 40% and 18%, respectively. On the other hand, for the third (symmetric) pattern, the enhancement is not so significant. The foregoing results indicate that the CSD should carefully be considered in the AP placement, particularly for WLANs that suffer from resource limitation and clients that are unsymmetrically distributed in the area under consideration.

VI. Conclusion

In this paper, we have developed a new model for R_{avg} estimation as well as a new scheme for WLAN AP placement with the consideration of CSD. We have shown through both simulation and analytical studies that the proposed model can provide a very efficient estimation for WLAN voice capacity and that this capacity can significantly be enhanced if we properly place the AP by using our new placement scheme, particularly when clients are unsymmetrically distributed in the WLAN area. It is expected that the work in this paper will contribute to the network planning and protocol design of future VoIP over WLANs.

Notice that the regular rate region pattern considered in this paper may be too simple to be realistic; therefore, one future work will be to examine the efficiency of our model for R_{avg} estimation based on a more realistic rate-region pattern that incorporates the effect of more factors like the channel fading and the shadowing effect. Another interesting future work will be to find a way to determine the required number of equal-sized squares for a given maximum-allowed estimation error of our model in voice-capacity estimation.

References

[1] P. Mockapetris, "Telephony's next act," *IEEE Spectr.*, vol. 43, no. 4, pp. 28–32, Apr. 2006.
[2] A. Kashyap *et al.*, "VoIP on wireless meshes: Models, algorithms and evaluation," in *Proc. IEEE INFOCOM*, 2007, pp. 2036–2044.
[3] F. Anjum *et al.*, "Voice performance in WLAN networks—An experimental study," in *Proc. IEEE GLOBECOM*, 2003, pp. 3504–3508.
[4] S. Garg *et al.*, "An experimental study of throughput for UDP and VoIP traffic in IEEE 802.11b networks," in *Proc. IEEE WCNC*, 2003, pp. 1748–1753.
[5] T. Patel, V. Ogale, S. Baek, N. Cui, and R. Park, *Capacity Estimation of VoIP Channels on Wireless Networks*, 2003. [Online]. Available: http://www.ece.utexas.edu/wireless/EE381K11Spring03/projects/11.3.pdf
[6] D. Hole and F. Tobagi, "Capacity of an IEEE 802.11b wireless LAN supporting VoIP," in *Proc. IEEE ICC*, 2004, pp. 196–201.
[7] S. Garg and M. Kappes, "Can I add a VoIP call?" in *Proc. IEEE ICC*, 2003, pp. 779–783.
[8] L. X. Cai, X. Shen, J. W. Mark, L. Cai, and Y. Xiao, "Voice capacity analysis of WLAN with unbalanced traffic," *IEEE Trans. Veh. Technol.*, vol. 55, no. 3, pp. 752–761, May 2006.
[9] Y. Zhang and B.-H. Soong, "Performance of mobile networks with wireless channel unreliability and resource insufficiency," *IEEE Trans. Wireless Commun.*, vol. 5, no. 5, pp. 990–995, May 2006.
[10] C. Tuduce and T. Gross, "A mobility model based on WLAN traces and its validation," in *Proc. IEEE INFOCOM*, 2005, vol. 1, pp. 664–674.
[11] C. Bettstetter, "On the minimum node degree and connectivity of a wireless multihop network," in *Proc. 3rd ACM Int. Symp. Mobile Ad Hoc Netw. Comput.*, 2002, pp. 80–91.
[12] *Part 11: Wireless LAN Medium Access Control (MAC) and Physical Layer (PHY) Specifications: High-Speed Physical Layer Extension in the 2.4/5 GHz Band*, ANSI/IEEE Std. 802.11b/a, 1999.
[13] R. P. Feynman, R. B. Leighton, and M. Sands, *The Feynman Lectures on Physics*. Reading, MA: Addison-Wesley, 2005.
[14] M. Hope and N. Linge, "Determining the propagation range of IEEE 802.11 radio LANs for outdoor applications," in *Proc. Local Comput. Netw.*, 1999, pp. 49–50.
[15] H. L. Bertoni, *Radio Propagation for Modern Wireless Systems*. Englewood Cliffs, NJ: Prentice–Hall, 2000.
[16] G. Marta, A. Cesar, and L. Albert, "Understanding individual human mobility patterns," *Nature*, vol. 453, no. 7196, pp. 779–782, Jun. 2008.
[17] M. Heger, "Human travel patterns surprisingly predictable," *IEEE Spectr.*, Jun. 2008.

Performance of Distributed Diversity Systems With a Single Amplify-and-Forward Relay

Himal A. Suraweera, *Member, IEEE*,
Diomidis S. Michalopoulos, *Student Member, IEEE*, and
George K. Karagiannidis, *Senior Member, IEEE*

***Abstract*—We study the error performance of the binary phase-shift keying (BPSK)-modulated distributed selection combining (SC) and distributed switched-and-stay combining (DSSC) schemes that utilize a single fixed-gain amplify-and-forward (AF) relay under Rayleigh fading conditions. The error performance of the distributed maximal ratio combining (MRC) is also investigated, which serves here as a benchmark. The numerical examples confirm that SC and DSSC offer a simpler substitute for MRC without much loss in performance. Moreover, we interestingly note that the performance of DSSC with a single fixed-gain AF relay is similar to that of DSSC with a single decode-and-forward relay, despite its relative simplicity.**

***Index Terms*—Amplify-and-forward (AF) relaying, error performance, selection combining (SC), switch-and-stay combining (SSC).**

Manuscript received March 23, 2008; revised June 26, 2008 and August 26, 2008. First published October 24, 2008; current version published May 11, 2009. The review of this paper was coordinated by Dr. J. Wu.

H. A. Suraweera is with the Center for Telecommunications and Microelectronics, School of Electrical Engineering, Victoria University, Melbourne, Vic. 8001, Australia (e-mail: himal.suraweera@vu.edu.au).

D. S. Michalopoulos and G. K. Karagiannidis are with the Wireless Communications Systems Group, Department of Electrical and Computer Engineering, Aristotle University of Thessaloniki, 54124 Thessaloniki, Greece (e-mail: dmixalo@auth.gr; geokarag@auth.gr).

Digital Object Identifier 10.1109/TVT.2008.2007798